Biosensors and Bioelectronics 141 (2019) 111481

Contents lists available at ScienceDirect

Biosensors and Bioelectronics

journal homepage: www.elsevier.com/locate/bios

A dual-transduction-integrated biosensing system to examine the 3D cell-culture for bone regeneration

Evgeny Kozhevnikov[a,1], Shupei Qiao[a,1], Fengtong Han[a], Wei Yan[b], Yufang Zhao[a], Xiaolu Hou[a], Alaka Acharya[a], Yijun Shen[a], Hui Tian[a], Haijiao Zhang[a], Xiongbiao Chen[c], Yuanchuan Zheng[d], Hongji Yan[e], Mian Guo[f,**], Weiming Tian[a,*]

[a] School of Life Science and Technology, Harbin Institute of Technology, Harbin, PR China
[b] Department of Cardiology, The First Affiliated Hospital of Harbin Medical University, Harbin, PR China
[c] Department of Mechanical Engineering, University of Saskatchewan, Saskatoon, Canada
[d] School of Chemistry and Chemical Engineering, Harbin Institute of Technology, Harbin, PR China
[e] Division of Glycoscience, Department of Chemistry, School of Engineering Sciences in Chemistry, Biotechnology and Health, KTH Royal Institute of Technology, Stockholm, Sweden
[f] Department of Neurosurgery, The Second Affiliated Hospital of Harbin Medical University, Harbin, PR China

ARTICLE INFO

Keywords:
Electrical impedance
Fluorescence imaging
Bone regeneration

ABSTRACT

Three-dimensional (3D) cell cultures developed with living cells and scaffolds have demonstrated outstanding potential for tissue engineering and regenerative medicine applications. However, no suitable tools are available to monitor dynamically variable cell behavior in such a complex microenvironment. In particular, simultaneously assessing cell behavior, cell secretion, and the general state of a 3D culture system is of a really challenging task. This paper presents our development of a dual-transduction-integrated biosensing system that assesses electrical impedance in conjunction with imaging techniques to simultaneously investigate the 3D cell-culture for bone regeneration. First, we created models to mimic the dynamic deposition of the extracellular matrix (ECM) in 3D culture, which underwent osteogenesis by incorporating different amounts of bone–ECM components (collagen, hydroxyapatite [HAp], and hyaluronic acid [HA]) into alginate-based hydrogels. The formed models were investigated by means of electrical impedance spectroscopy (EIS), with the results showing that the impedances increased linearly with collagen and hyaluronan, but changed in a more complex manner with HAp. Thereafter, we created two models that consisted of primary osteoblast cells (OBs), which expressed the enhanced green fluorescent protein (EGFP), and 4T1 cells, which secreted the EGFP-HA, in the alginate hydrogel. We found the capacitance (associated with impedance and measured by EIS) increased with the increases in initial embedded OBs, and also confirmed the cell proliferation over 3 days with the EGFP signal as monitored by the fluorescent imaging component in our system. Interestingly, the change in capacitance is found to be associated with OB migration following stimulation. Also, we show higher capacitance in 4T1 cells that secret HA when compared to control 4T1 cells after a 3-day culture. Taken together, we demonstrate that our biosensing system is able to investigate the dynamic process of 3D culture in a non-invasive and real-time manner.

1. Introduction

Bone is a tissue that undergoes constant remodeling to maintain its healthy state and holds scar-free, self-healing abilities. However, critical bone defects, such as those caused by trauma, tumor-removal surgery, and osteoporosis, are non-uniform and require surgical intervention. Over 4 million bone transplants and grafts are performed every year around the world (Danikas et al., 2002). Alternatively, tissue regeneration-based approaches have emerged, which involve the development of scaffolds with growth factors and/or cells to promote the healing of critical bone defects (Yan et al., 2018). Bone consists of an exceptionally abundant ECM produced by osteoblasts (OBs) with

* Corresponding author.
** Corresponding author.
E-mail addresses: guomian@hrbmu.edu.cn (M. Guo), tianweiming@hit.edu.cn (W. Tian).
[1] Equal contribution.

https://doi.org/10.1016/j.bios.2019.111481
Received 18 April 2019; Received in revised form 31 May 2019; Accepted 26 June 2019
Available online 27 June 2019
0956-5663/

~60% inorganic calcium phosphate minerals (primarily HAp) and 30% organic materials (mainly collagen; Doblare and Garcia, 2003). The ECM is known to exert its functions by supporting living cells, but it also actively provides biological and mechanical stimuli and contributes to bone remodeling (Alford et al., 2015). 3D solutions enable researchers to investigate the various biological processes that involve ECM deposition and remodeling by cultured cells *in vitro*, including osteogenesis. Despite recent advances in this area, it can still be challenging to monitor or obtain appropriate information on the bone-regeneration process, including the secreted components of the ECM that are associated with cell growth and functions, particularly in real time. The existing monitoring techniques are typically reliant on microscopy-based technologies to examine the samples collected at a certain period. These techniques suffer from limited sensitivity, selectivity, and stability, and they are also cumbersome and time-consuming. When cell-culture medium is involved, the plethora of nonspecific binding proteins and interfering compounds are also involved. As a result, there is a great desire for biosensing systems that are able to monitor real-time ECM formation and cell growth/functions for bone regeneration in 3D culture.

EIS has a broad range of applications, including in cell biology, to monitor real-time cellular changes caused by proliferation (Lee et al., 2014), apoptosis (Arndt et al., 2004), or cell–cell interactions (Saffitz and Kleber, 2004). Recently, biosensors measuring impedance have been used to primarily detect changes in cell number in 3D culture; this is done in conjunction with optical images captured at the end of the cell-culture process (Lee et al., 2016; Zhang et al., 2018). The data obtained at different time points using different methods may not be consistent when describing the dynamic cell-culture process. Further, to date, no data have been reported that have explored the use of EIS to detect the formation of ECM in 3D cell culture. The ECM continuously undergoes changes as living cells grow and function; in this regard, the combination of visual optical methods and EIS in real-time has numerous advantages when compared to those methods that use individual biosensing techniques and those applied at different time points (as noted above). In addition, the data obtained at the same time points, but by employing different methods, allow for complementary interpretations of the cell-culture process, which is critical for complex dynamic systems, such as the bone-regeneration process being investigated in the present study. Previously, we revealed that EIS impedance gradually increased following bone healing in a rabbit model of a critical bone defect (Kozhevnikov et al., 2016). We revealed how the electrical impedance was positively or negatively correlated with the amount of collagen and HAp present in the fracture area. However, a firm explanation on how electrical impedance correlates to the changes of deposited bone ECM has yet to be provided.

This paper reports a dual-transduction-integrated biosensing system that can simultaneously trace ECM formation and cell behavior in 3D cell culture. We demonstrated that EIS impedance is responsive to changes in the organic components of the ECM. Furthermore, we used adenovirus to transfect the primary OBs in rats with EGFP plasmid and then encapsulated the cells in alginate scaffolds. With the dual-transduction-integrated biosensing system, we demonstrated that it is feasible to simultaneously examine ECM formation and cell growth. Moreover, was observed significant advantages associated with using the biosensor while investigating the electrical stimulation of 3D cell-culture systems.

2. Materials and methods

The dual-transduction-integrated biosensing system is schematically presented in Fig. 1, as are the designed verification experiments. We first created bone-regeneration models by adding the bone ECM components – i.e., collagen, HAp, and HA, respectively – into alginate, which were then gelled by means of $CaCl_2$. The formed models were investigated by EIS and scanning electron microscopy (SEM). To investigate the bone-regeneration 3D cell-culture system, the cells were isolated and cultivated, after which point, they were infected with an adenovirus that can express EGFP. Then, the cells were homogeneously suspended in alginate solution. After gelling the hydrogel in a dish containing measurement electrodes, the 3D cell-culture system was simultaneously examined by EIS and fluorescence microscopy. A detailed description of the materials and methods used in this study can be found in the SI Materials and Methods section.

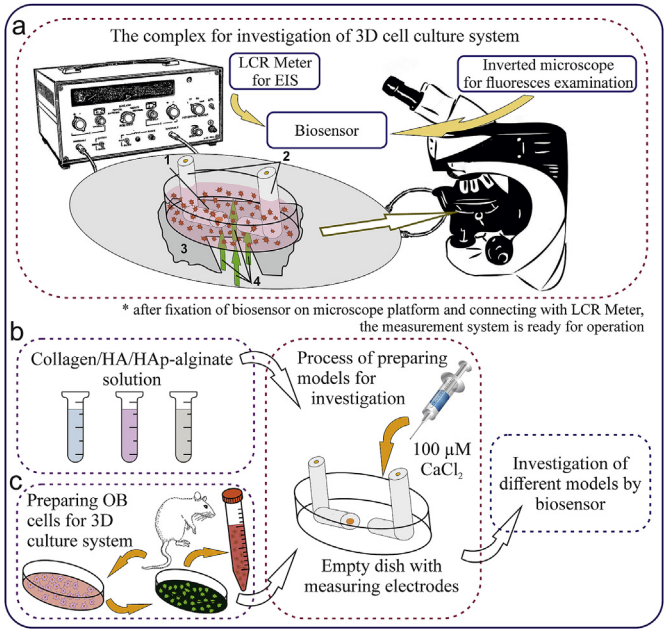

Fig. 1. (a) Schematic of the dual-transduction-integrated biosensing system, which primarily consists of an LCR meter to detect impedance and an inverted microscope to detect fluorescence. (b) Bone-regeneration models of different bone ECM (collagen/HAp/HA) components and their examination via EIS and SEM. (c) 3D cell culture and its examination using the dual-transduction-integrated biosensing system.

3. Results and discussion

3.1. Effect of the changes in the bone matrix on bone impedance

Alginate hydrogel (ionically crosslinked with $CaCl_2$) featuring various amounts of the elements that comprise bone ECM (collagen/HAp/HA) was used as a model to mimic the ECM deposited by OBs in bone tissue. A series of EIS measurements was conducted (frequencies: 1, 1.2, 1.5, 2, 2.5, 3, 4, 5, 6, 7.5, and 10 kHz; V = 0.1 V) on the hydrogels described above to measure the electrical impedance and to determine the phase corresponding to the observed ECM changes. Thereafter, the hydrogel microstructure was examined by SEM.

3.1.1. Effect of collagen concentration on impedance change

The impedance of the collagen–alginate scaffolds increased stepwise in proportion with the amount of collagen contents present. The impedance values ranged from 1.375 to 1.875 kΩ; that is, increases in collagen ranging from 2% to 25% increased the impedance by ~0.5 kΩ (Fig. 2a). The phase characteristic is linear, which indicates the changes in the active and capacitive components of impedance; however, the values for scaffolds containing 23% collagen content are out of sequence with the other scaffolds considered (Fig. 2b). Cross-sectional images of the collagen–alginate scaffolds (Fig. 2c–i) indicated that all samples had an evenly distributed porous structure, suggesting good interconnectivity. The size of pores in the scaffolds also tended to increase with increasing collagen content (2%, 5%, 13%, 15%, 20%, 23%, 25%). This increase is particularly evident at scaffold collagen

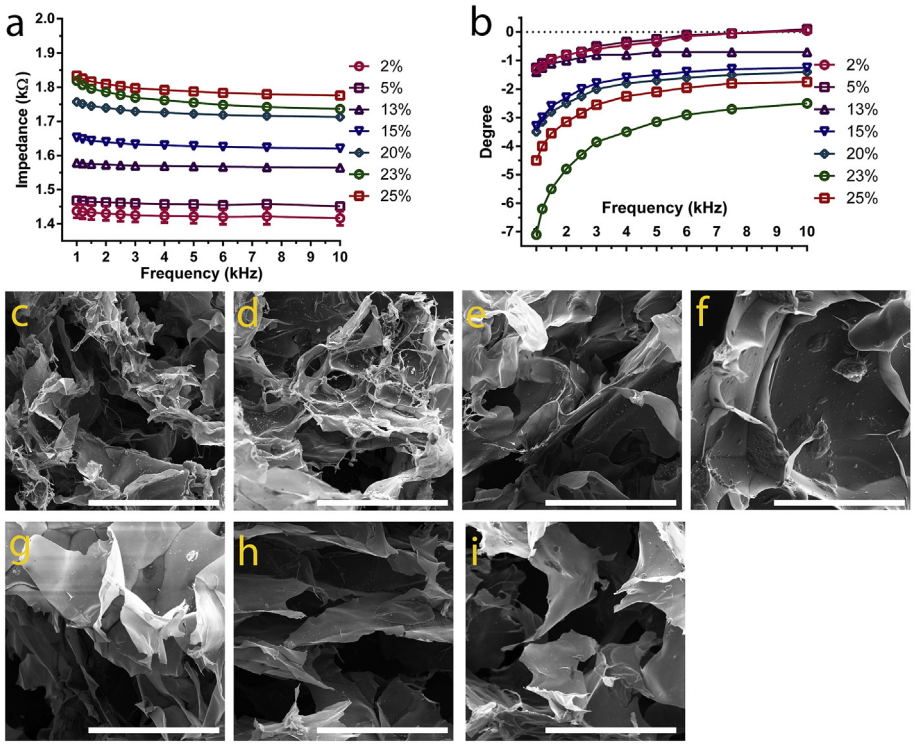

Fig. 2. Results of (a, b) EIS and (c–i) SEM for collagen–alginate scaffolds. EIS data are presented as impedance (kΩ) and phase (degree). SEM micrographs show the pore size of the collagen–alginate scaffolds with different collagen content (c, 2%; d, 5%; e, 13%; f, 15%; g, 20%; h, 23%; and i, 25%). Scale bar: 250 μm.

concentrations of 20% or more (20%, 23%, 25%).

3.1.2. Effect of HA concentration on impedance change

The impedance and phase of the HA–alginate scaffold groups were very similar to those of the collagen–alginate scaffolds; the impedance values also demonstrated step-wise increases in proportion to HA content. The impedance values fell between the range of 1.2 kΩ and 1.7 kΩ; that is, an increase in HA concentration from 0.5% to 10% increased the impedance by ~0.4 kΩ (Fig. 3a). The phase characteristic was also linear and described the change in the active and capacitive components of impedance (Fig. 3b). Cross-sectional images of HA–alginate scaffolds (Fig. 3c–f) showed that all samples had an evenly distributed and open porous structure, suggesting good interconnectivity. The size of the pores in the samples also tended to increase with increasing amounts of HA in the scaffold (0.5%, 1%, 5%, 10%).

3.1.3. Effect of HAp concentrations on impedance change

An increase in impedance was observed with increasing concentrations of HAp in the scaffold. However, this increase was gradual at concentrations of 10%, 15%, and 20%, but it became very rapid at 25%; that is, at HAp concentrations of 10%, 15%, and 20%, the impedance ranged from 1.25 to 1.375 kΩ, but at HAp content of 25%, the increases occurred very rapidly at an initial frequency of 1 kHz to > 2.25 kΩ (Fig. 4a). This is due to a critical increases in calcium, which is of poor conductivity and also responsible for the large electrical impedance in bone as compared to other tissues. The phase characteristic

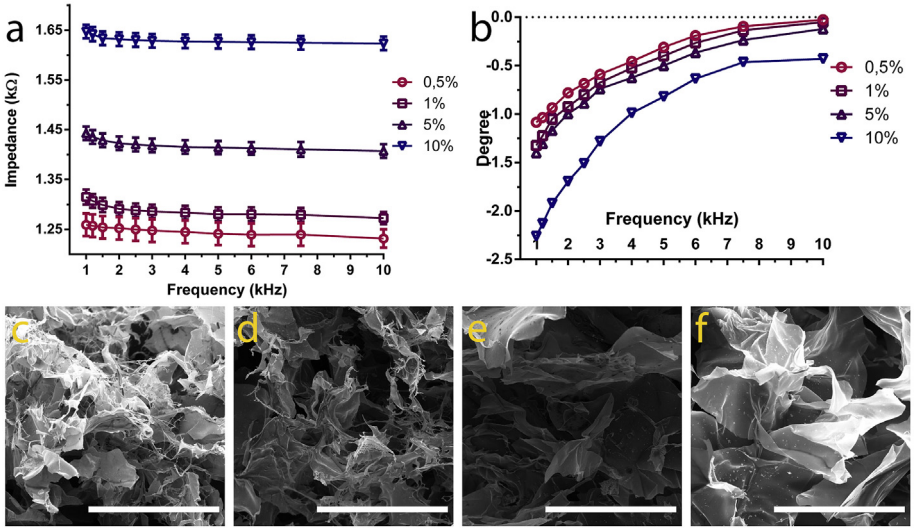

Fig. 3. Results of (a, b) EIS and (c–f) SEM for HA–alginate scaffolds. EIS data are presented as impedance (kΩ) and phase (degree). SEM micrographs show the pore size of the HA–alginate scaffolds with different HA content (c, 0.5%; d, 1%; e, 5%; and f, 10%). Scale bar: 250 μm.

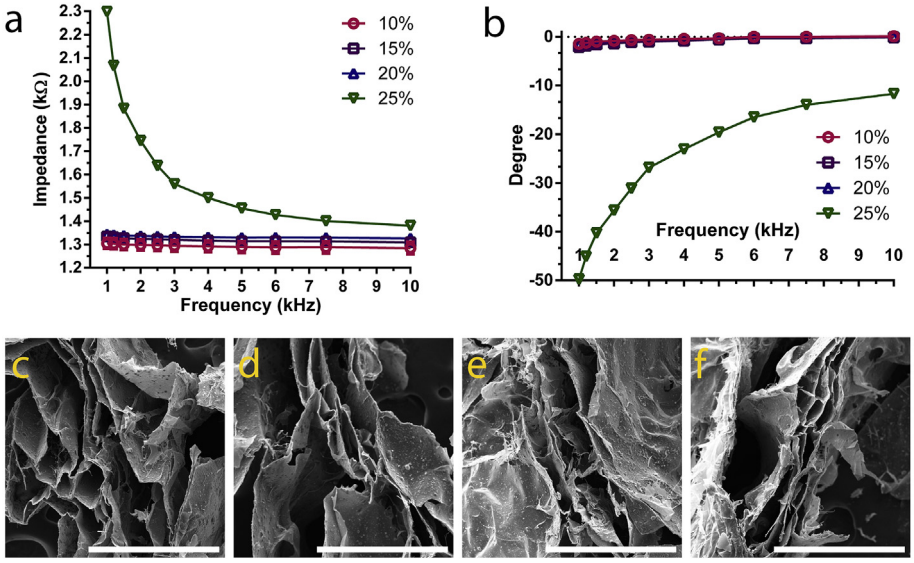

Fig. 4. Results of (a, b) EIS and (c–f) SEM for HAp–alginate scaffolds. EIS data are presented as impedance (kΩ) and phase (degree). SEM micrographs show the pore size of the HAp–alginate scaffolds with different HAp content (c, 10%; d, 15%; e, 20%; and f, 25%). Scale bar: 250 μm.

also changed rapidly (Fig. 4b). SEM micrographs and the pore size of the Hap-alginate scaffold with different HAp concentrations (10%, 15%, 20%, 25%) are presented in Fig. 4c–f.

The HAp–alginate scaffolds show some similarities to the previous two models, depending on the amount of HAp in the scaffold. Briefly, the structure of the HAp–alginate scaffolds with different amounts of HAp is uniform, and the size of the pores in the different scaffolds is almost equal. The structure of the HAp–alginate scaffold is similar with those of the collagen–alginate and HA–alginate scaffolds at low concentrations of the major elements (when HAp–alginate scaffolds contain 10% HAp, collagen–alginate scaffolds contain 2% collagen, and HA–alginate scaffolds contain 0.5% or 1% HA).

3.1.4. Assessing scaffold formation for 3D culturing by EIS

Increasing the amount of collagen/HAp/HA in the alginate scaffolds leads to changes in the impedance of these bone-regeneration models. The collagen and HA content of the scaffolds greatly affects the capacitance component of the impedance measurement. The SEM results showed that pore size noticeably increased with the collagen and HA content present in the scaffold. The pores in the scaffold represent capacitors that are associated with geometric size and dielectric filler. Compared with collagen, HAp has a greater impact on the active component of impedance. HAp also increased the resistance of the pore walls and connections without exerting a specific influence on pore size and pore orientation in the scaffolds. The results were confirmed by SEM, which exhibited a similar shape, size, and orientation as the pores in the HAp–alginate scaffolds regardless of HAp content. The impedance and phase angle complemented each other and were used to indicate the relative (rather than absolute) amounts HAp, collagen, and HA in the scaffolds.

Nevertheless, no convincing data about the impact of elements on the structure of the system were reported, despite the importance of the structure of the system being repeatedly noted (Foster and Schwan, 1995). Collagen formation results from OB cell secretions. In the next stage of bone-tissue development, HAp nanocrystals are deposited on collagen fibers, thus strengthening the bone (Currey, 2013). At the same time, increasing amounts of HA are observed in the ECM with cell proliferation and migration. All of these elements of the ECM have a direct impact on the state and development of bone tissue in the organism. Our results show that the effects of collagen/HAp/HA on its surroundings can be detected. Cell-secretion products in bone-like 3D cell culture systems also interact with the systems and change their general states and structures. Cell densities will define this influence; however, changes in the impedance of these systems occurs with a high cell density, but will change quite smoothly in systems with a low cell density. Hence, we can monitor the bone-cell secretion of collagen, HAp, and HA, as well as their influence on 3D cell-culture systems by applying EIS.

3.2. Monitoring 3D culture systems using the biosensing system

Given the identified relationship between the bone-matrix components and the measured impedance, we tested whether the cell behavior of OB also has an impact on impedance due to cell proliferation, cell migration, and cell secretion, as each of these processes can affect the structure and amount of components present in the ECM. To investigate cell behavior of OBs in the 3D scaffolds (Fig. 1c), a bone-regeneration 3D cell-culture system was formed and examined. EIS and optical fluorescence investigations were simultaneously carried out at predefined time points. The dependence of capacitance on cell states in the system was detected at frequencies of 1, 1.2, 1.5, 2, 2.5, 3, 4, 5, 6, 7.5, and 10 kHz (V = 0.1 V).

3.2.1. 3D culture systems without cells and their characterization

We used the EIS technique to characterize the impedance of bone regeneration 3D cell-culture systems over a period of 3 h. Briefly, 100 μM of $CaCl_2$-buffered Dulbecco Modified Eagle's Medium (DMEM) culture medium were added to the alginate solution with encapsulated OB cells (10^5 cells/mL); then, the capacitance was measured at a frequency of 4 kHz every 0.5 h for 3 h. Concurrent optical fluorescence examinations were carried out at 0, 0.5, 1, and 3 h.

The capacitance gradually increased over the course of the 3-h experiment (Fig. S2a). Significant differences ($P < 0.05$) between the capacitance values at the start of the experiment and after 0.5 h, 1 h, and 3 h of investigation are noted (Fig. S2b). However, all capacitance changes after 1 h are minor. Within the first hour, the 3D cell-culture system forms via gelatinization of an alginate solution by CaCl2-buffered DMEM culture medium. After 0.5 h, the process is incomplete and most of the 3D scaffold is not formed. This causes profound changes in capacitance during the first hour. The subsequent changes in capacitance can be explained by several factors. First, due to cell viability, the level of capacitance did not decrease and preserved its positive dynamics. Briefly, damage to the cell membrane causes a reduction in capacitance, and infiltration of intracellular fluid into the environment

leads to increases in the conductivity in nearby areas (Lee et al., 2016). Second, cell adhesion (resulting from the conversion of cellular contacts) strengthens the relationship between cells and the scaffold, thereby creating new barriers to the passage of an electrical signal. Third, cell proliferation and migration also result in increased capacitance (Arias et al., 2010). Fig. S2b shows fluorescence images of cells at the same time points as the capacitance measurements were captured; however, it was quite difficult to ascertain whether a significant increase in cell density occurred within the system. Hence, we surmise that the gelatinization of the alginate solution (the formation of a 3D scaffold) affects the capacitance in the early stages of creating a 3D culture system, and that cell adhesion, proliferation, and migration do as well, but to a lesser extent. Consequently, we can monitor the scaffold-formation process and optimize the impact of forming factors by measuring the changes in electrical impedance of the 3D culture system. Previously published experiments have not considered EIS data as a source of information when examining the formation of the structure and degree of maturity of 3D scaffolds (Lee et al., 2016).

3.2.2. 3D cell culture systems with living cells and their characterization

Various densities of OB cells (10^2, 10^3, 10^4, and 10^5 cells/mL) were encapsulated in alginate hydrogel and cultured for 72 h to evaluate cell proliferation in the 3D system. The results of this simultaneous investigation are presented in Fig. 5a–d. Increasing cell density is associated with significant increases in capacitance in each 3D culture system. At the same time, the fluorescence images also identified the development of 3D cell-culture systems over time in each of the groups featuring different cell densities. Over the entire experimental period, increasing electrical impedance and cell fluorescence were simultaneously recorded for each 3D system. This demonstrates that we can use two methods at the same time to investigate the dynamically variable state of cell growth in 3D cell-culture systems. From the results shown in Fig. 5, it was evident that the capacitance observed after 72 h of cultivation was equal to the capacitance for the subsequent discharge of cell density (capacitance after 72 h of 10^2 cells/mL equals the capacitance at 0 h of 10^3 cells/mL, etc.). These results suggest that the capacitance in the cell-culture system not only depends on the number of cells, but it also hinges on other states, including cell behavior, ECM changes, and cell growth.

To further confirm this finding, 4T1 cells that could secrete EHMW–HA were cultured in our 3D cell-culture system to detect whether HA secretion had an impact on impendence. As shown in Fig. 6a, all groups (both the control and overexpressed HA groups) were observed to have increased capacitance. In the group that demonstrated secretion of high-molecular-weight HA, the level of capacitance was higher than in the first group, but the fluorescence images were similar. The highest level of capacitance in the second group was associated with the release of HA by 4T1 cells. Based on these results, we demonstrated that EIS is an effective method through which to monitor cell secretion in the 3D cell-culture system.

In order to test our biosensing system's efficacy when simultaneously monitoring cell migration and impendence, we carried out a series of electrical stimulation experiments. Briefly, the OBs were cultured in 3D bone-regeneration systems, which were divided into three groups (Group 1: 1 V/cm; Group 2: 3 V/cm; Group 3: 5 V/cm). Before and after the electrical stimulation, the cells were investigated using our biosensing system. As shown in Fig. 6b–c, all groups demonstrated an increase in capacitance in the 3D cell-culture system at the end of the study. The largest increase in capacitance was detected in Group 2. The values from Groups 1 and 3 were very similar, but less than that of the control group. The cell fluorescence images indicated that there was more effective stimulation in Group 2, a strong dispersion of cells in Group 3 (excessive stimulation), and insufficient stimulation in Group 1, with a small output of cells from the initial area. Based on these studies, we were able to determine the most effective mode of cell stimulation and subsequently investigated the complex change in the state of the 3D culture system over time for each group. Thus, it was impossible to accurately assess the results of 3D cell-culture stimulation using only one research method. Namely, with equal capacitance values, the optical method will play a crucial role in the study of 3D models. Through fluorescent images, we are able to capture information about cell location and their orientation in the structure of the scaffold. The general assessment of the 3D model state and cells activities is given using impedance measurements. By combining these two methods simultaneously, we can obtain complementary information on the dynamics of 3D cell-culture systems.

Also, our biosensing system was used to monitor other cell-culture systems with different cell lines (OBs, raw 264.7, and 4T1 cells). It was observed that capacitance depended on the cell line; the highest value was observed for the 4T1 cell line and the lowest for the raw 264.7 cell line (Fig. S3).

Accordingly, EIS changes in bone-regeneration 3D cell-culture systems should not only be associated with cell proliferation and migration. Throughout the course of their life cycle, cells secrete various substances that affect the environment and structure of the 3D cell-culture system, as well as the cells' interactions with the system. Over time, the influence of cellular secretions increases and leads to more drastic changes in the scaffold structure, environment, and interactions. These dynamic, fast, and inconspicuous processes can be simultaneously recorded by EIS and examined by an optical imaging technique. Only by applying an integrated approach to research is it possible to obtain high-quality and complete data. Fluorescence investigations of 3D systems can be very similar – equal numbers of cells are present in the two 3D systems, but the actual state of each 3D cell-culture system will differ and can be assessed by EIS (as well, the impedance of these two systems will also be different); in other words, the EIS characteristics of each 3D cell-culture system are unique. At the same time, there may be similar impedance values for the two individual systems, but their fluorescence may be different. This dual-transduction biosensing system can provide a complementary assessment of the bone-regeneration state in a 3D cell-culture system. Namely, in addition to assessing the number of cells and their distribution in the 3D cell-culture systems, the dual-transduction biosensing system can detect the impacts of different ECM–cell interactions on the state systems. By doing so, our dual-transduction biosensing system represents a significant improvement over the reported studies where either EIS or optical methods were applied (Jeong et al., 2012; Lee et al., 2016).

In addition to the processes that lead to increased impedance, the processes that reduce impedance also take place during system development. First, electrical impedance decreases due to scaffold degradation; this is associated with the destruction of the structure and breakage of linkages within the system. Second, damage to the cell membrane can result in intracellular fluid leakage into the environment. This destruction of the cell membrane causes decreased capacitance. Intracellular fluid (due to its chemical composition) increases conductivity, thereby reducing resistance. Based on the results of this investigation (the lack of sharp drops on the graphs), we assume that the impact of the above factors was limited and had no significant effect on our studies. At the same time, sharp drops in the capacitance value would indicate problems in the development of the 3D culture system. Our point here is that the above reasons for changes in electrical impedance, as well as the inner processes in the 3D culture, cannot be detected by cell fluorescence. Therefore, by combining these two methods, we can accurately and completely describe the process of cell-culture system development.

4. Conclusions

In this study, we developed a dual-transduction-integrated biosensing system and demonstrated how it can monitor the dynamic changes of a 3D culture in real time, as living cells consistently rebuild their own ECM. We first focused on the bone ECM components collagen, HAp, and

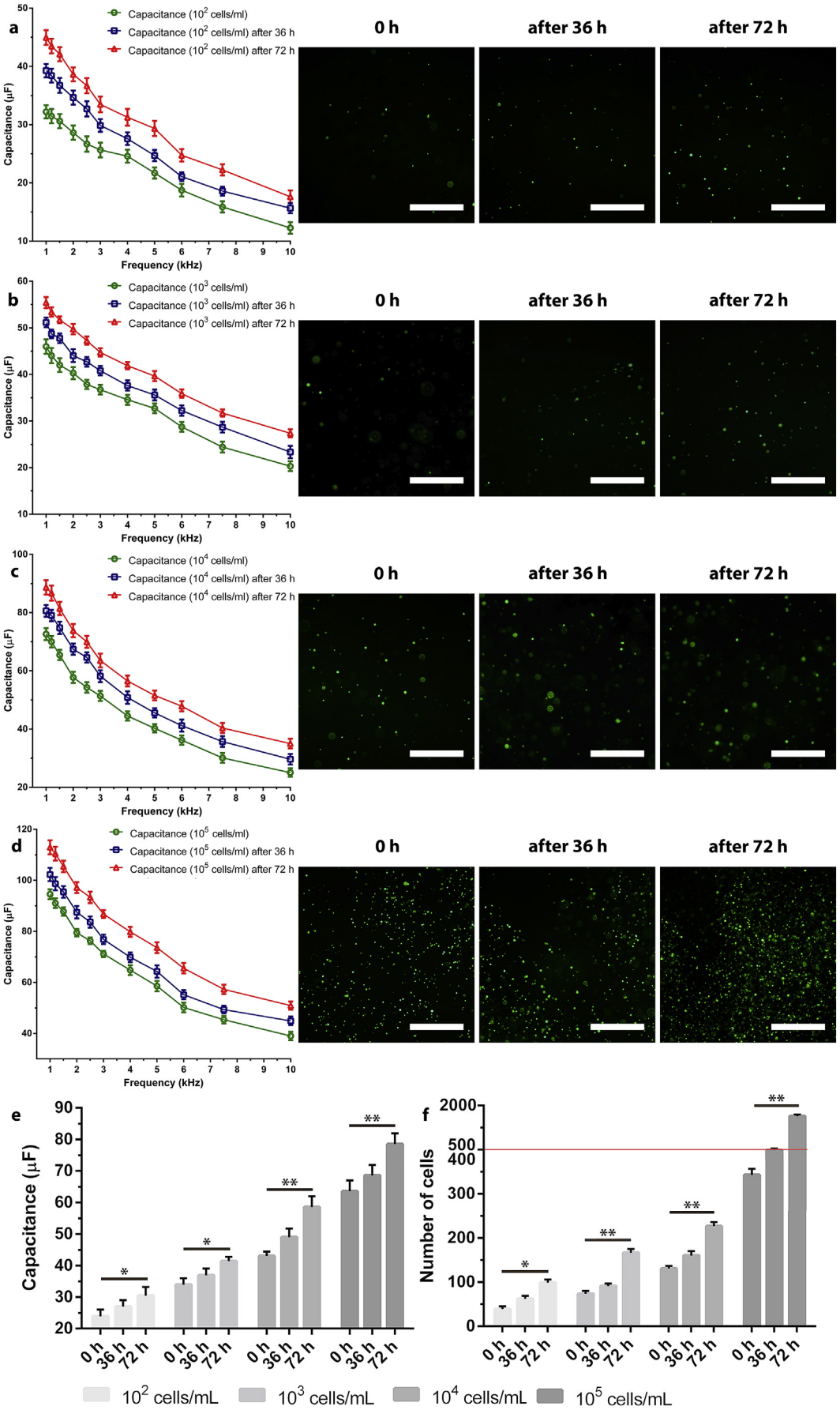

(caption on next page)

Fig. 5. Alginate solution with encapsulated OB cells following gelatinization was studied over 72 h. (a–d) The dependence of capacitance on frequency for various 3D cell-culture systems (a, 10^2 cells/mL; b, 10^3 cells/mL; c, 10^4 cells/mL; d, 10^5 cells/mL) was determined at range of frequencies. Also presented are results of the simultaneously captured fluorescent optical images with corresponding cell densities. Scale bar: 1 mm. (e) The capacitance of the bone-like 3D cell-culture systems with different cell numbers (at 4 kHz), and (f) the number of cells observed at the control time points, as calculated using ImageJ.

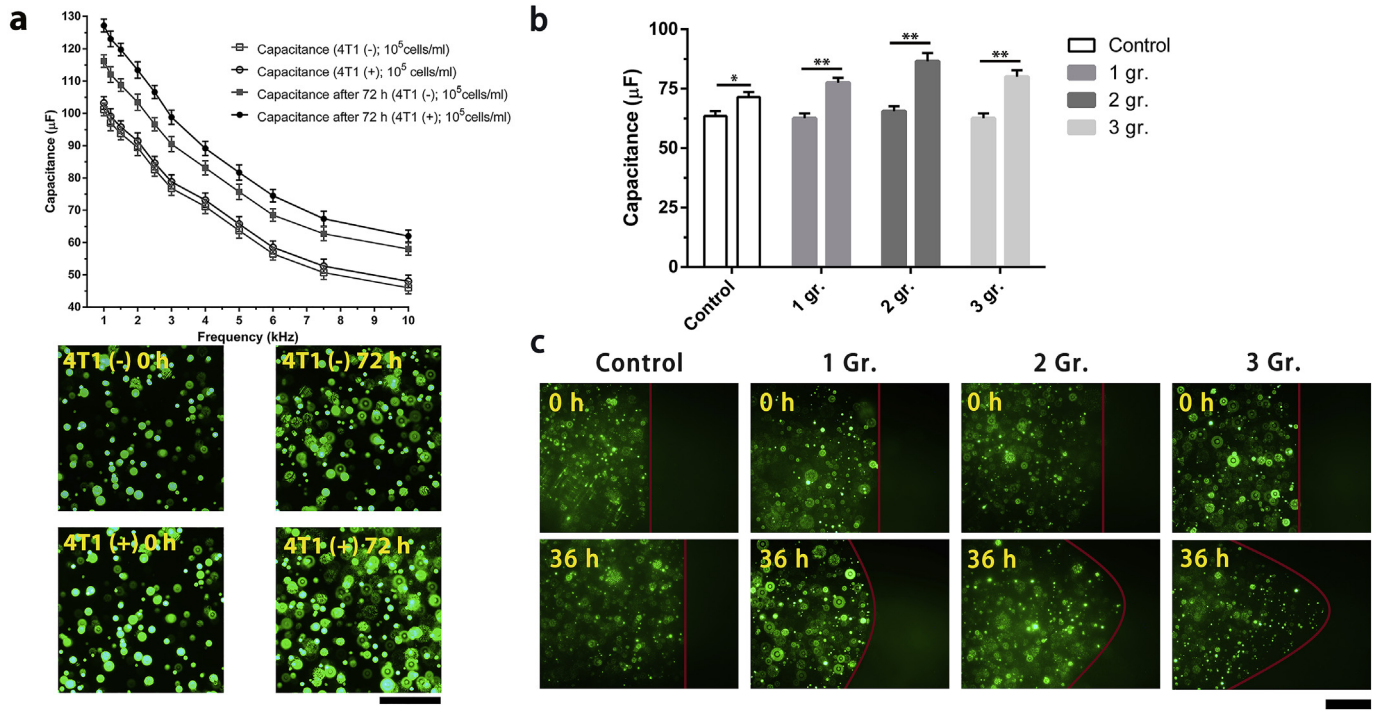

Fig. 6. (a) The capacitance of the 4T1 cells (10^5 cells/mL) with/without the secretion of HA (+)/(−), measured after gelatinization and at 72 h. Fluorescence also was detected for two groups. Scale bar: 0.5 mm. (b) Capacitance of the bone-like 3D cell culture systems (OB; 10^5 cells/mL) before and after stimulation (at 4 kHz); (c) simultaneous fluorescent optical images (scale bar: 1 mm).

HA and showed how the impedance measured by EIS can be used as a parameter to detect and quantify the components in a 3D scaffold. Second, we encapsulated OBs in alginate hydrogel and then examined the general state of the 3D cell-culture system, including cell behavior and cell secretion, by both EIS and fluorescence imaging in real time. We demonstrated that the EIS and fluorescence imaging results are complementary and that the integration of EIS and optical fluorescence techniques into a biosensing system can be leveraged to investigate 3D cell-culture systems. We finally used the system to monitor a model that we established, which consists of living cells that expresses HA ECM, to mimic how living cells and associated cell behaviors simultaneously operate to form the ECM. By using such a biosensing system, cell behavior–including the impacts of cell proliferation and secretion in 3D culture systems – can be monitored and evaluated in a non-invasive way and in real-time. It is noted that some processes in the 3D culture system could only be detected by EIS, while optical imaging techniques allow for the visualization of cell growth and distribution. As such, by combining the two different – yet complementary – techniques, the biosensing system employed in the present study represents a significant advancement in biosensing and regenerative medicine.

CRediT authorship contribution statement

Evgeny Kozhevnikov: Investigation, Conceptualization, Data curation, Writing - original draft, Writing - review & editing. **Shupei Qiao:** Investigation, Data curation, Writing - original draft, Writing - review & editing. **Fengtong Han:** Investigation. **Wei Yan:** Writing - review & editing, Formal analysis. **Yufang Zhao:** Writing - review & editing, Formal analysis. **Xiaolu Hou:** Writing - review & editing, Formal analysis. **Alaka Acharya:** Writing - review & editing, Formal analysis. **Yijun Shen:** Investigation. **Hui Tian:** Investigation. **Haijiao Zhang:** Investigation. **Xiongbiao Chen:** Writing - original draft, Writing - review & editing. **Yuanchuan Zheng:** Writing - review & editing, Formal analysis. **Hongji Yan:** Writing - original draft, Writing - review & editing. **Mian Guo:** Methodology, Resources, Writing - review & editing. **Weiming Tian:** Project administration, Resources, Writing - review & editing.

Acknowledgements

Research is supported by National Natural Science Foundation of China (grants 51773050, 21407036, 81773161, 81572472), Natural Science Foundation of Heilongjiang Province of China (No. B2015005), Natural Science and Engineering Research Council of Canada.

Appendix A. Supplementary data

Supplementary data to this article can be found online at https://doi.org/10.1016/j.bios.2019.111481.

References

Arndt, S., Seebach, J., Psathaki, K., Galla, H.-J., Wegener, J., 2004. Bioelectrical impedance assay to monitor changes in cell shape during apoptosis. Biosens. Bioelectron. 19, 583–594.
Arias, L.R., Perry, C.A., Yang, L., 2010. Real-time electrical impedance detection of cellular activities of oral cancer cells. Biosens. Bioelectron. 25 (10), 2225–2231.
Alford, A.I., Kozloff, K.M., Hankenson, K.D., 2015. Extracellular matrix networks in bone remodeling. Int. J. Biochem. Cell Biol. 65, 20–31.
Currey, J.D., 2013. Bones: Structure and Mechanics. Princeton University Press.
Danikas, D., Theodorou, S.J., Stratoulias, C., Constantinopoulos, G., Ginalis, E.M., 2002. Hernia through an iliac crest bone-graft donor site. Plast. Reconstr. Surg. 110 (6),

1612–1613.
Doblare, M., Garcia, J.M., 2003. On the modelling bone tissue fracture and healing of the bone tissue. Acta Cient. Venez. 54 (1), 58–75.
Foster, K.R., Schwan, H.P., 1995. Dielectric properties of tissues. Chapter 1 (pages 25-102. In: Polk, C., Postow, E. (Eds.), Handbook of Biological Effects of Electromagnetic Fields, second ed. CRC Press, Boca Raton, FL.
Jeong, S.H., Lee, D.W., Kim, S., Kim, J., Ku, B., 2012. A study of electrochemical biosensor for analysis of three-dimensional (3D) cell culture. Biosens. Bioelectron. 35 (1), 128–133.
Kozhevnikov, E., Hou, X., Qiao, S., Zhao, Y., Li, C., Tian, W., 2016. Electrical impedance spectroscopy–a potential method for the study and monitoring of a bone critical-size defect healing process treated with bone tissue engineering and regenerative medicine approaches. J. Mater. Chem. B 4 (16), 2757–2767.
Lee, S., Han, N., Lee, R., Choi, I., Park, Y., Shin, J., Yoo, K., 2016. Real-time monitoring of 3D cell culture using a 3D capacitance biosensor. Biosens. Bioelectron. 77, 56–61.
Lee, E.J., Wi, H., McEwan, A.L., Farooq, A., Sohal, H., Woo, E.J., Seo, J.K., Oh, T.I., 2014. Design of a microscopic electrical impedance tomography system for 3D continuous non-destructive monitoring of tissue culture. Biomed. Eng. Online 13, 142.
Saffitz, J.E., Kleber, A.G., 2004. Effects of mechanical forces and mediators of hypertrophy on remodeling of gap junctions in the heart. Circ. Res. 94 (5), 585–591.
Yan, H.J., Casalini, T., Hulsart-Billstrom, G., Wang, S., Oommen, O.P., Salvalaglio, M., Larsson, S., Hilborn, J., Varghese, O.P., 2018. Synthetic design of growth factor sequestering extracellular matrix mimetic hydrogel for promoting in vivo bone formation. Biomaterials 161, 190–202.
Zhang, N., Stauffer, F., Simona, B.R., Zhang, F., Zhang, Z.M., Huang, N.P., Vörös, J., 2018. Multifunctional 3D electrode platform for real-time in situ monitoring and stimulation of cardiac tissues. Biosens. Bioelectron. 112 (30), 149–155.